Fabrication of Tunable Janus Microspheres with Dual Anisotropy of Porosity and Magnetism

ARTICLE *in* LANGMUIR · APRIL 2013

Impact Factor: 4.46 · DOI: 10.1021/la400053g · Source: PubMed

4 AUTHORS:

Yin Ning
The University of Sheffield
9 PUBLICATIONS **99** CITATIONS
SEE PROFILE

Chaoyang Wang
South China University of Technology
118 PUBLICATIONS **1,799** CITATIONS
SEE PROFILE

To Ngai
The Chinese University of Hong Kong
94 PUBLICATIONS **1,304** CITATIONS
SEE PROFILE

Zhen Tong
South China University of Technology
197 PUBLICATIONS **3,752** CITATIONS
SEE PROFILE

Langmuir

Article

pubs.acs.org/Langmuir

Fabrication of Tunable Janus Microspheres with Dual Anisotropy of Porosity and Magnetism

Yin Ning,[†] Chaoyang Wang,*[,†] To Ngai,*[,‡] and Zhen Tong[†]

[†]Research Institute of Materials Science, South China University of Technology, Guangzhou 510641, China

[‡]Department of Chemistry, The Chinese University of Hong Kong, Shatin, N.T., Hong Kong, China

Supporting Information

ABSTRACT: This work presents a facile approach to produce a novel type of Janus microspheres with dual anisotropy of porosity and magnetism based on Pickering-type double emulsion templates. A stable aqueous Fe_3O_4 dispersion-in-oil-in-water ($W_F/O/W$) double Pickering emulsion is first generated by using hydrophobic silica and hydrophilic mesoporous silica particles as stabilizers. Janus microspheres with multihollow structure possessing magnetite nanoparticles concentrated on one side of the microspheres are obtained after polymerization of the middle oil phase of the double emulsion under a magnetic field. The resultant Janus microspheres are characterized by optical microscopy, scanning electron microscopy (SEM), and energy-dispersive X-ray analysis (EDX). Moreover, we have systematically investigated the influences of Fe_3O_4 particle concentration, hydrophobic silica particle content, and volume ratio of the inner water phase to middle oil phase (W_F/O) on the double emulsion formation and consequently on the structure of the resulting Janus microspheres. Our results show that the distribution of the multihollow structures within the prepared microspheres can be accurately tailored by adjusting the ratio of W_F/O. In addition, the obtained Janus microsphere can be fairly orientated under a magnetic field, making them a potential candidate for synthesizing Janus membrane.

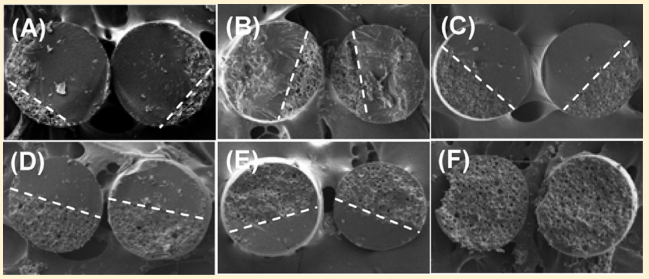

INTRODUCTION

Janus particles, whose two sides or surfaces are different in terms of chemical and/or physical properties, have gained significant attention in recent years due to their novel morphologies and unique natures, endowing them with diverse potential applications such as switchable display devices,[1] interface assembles,[2−5] optical sensors,[6] and anisotropic building blocks for complex structures.[7−11] During the past decade, a number of methods, including surface coating,[12−16] biphasic electrified jetting,[17] self-assembly,[18−22] *in situ* "click chemistry",[23] microfluidic technique,[24−26] and Pickering emulsion template,[27−34] have been developed for the preparation of Janus particles. Among them, the Pickering emulsion template has received particular interest because it provides the feasibility to control the geometry of the Janus particles, i.e., the relative areas of their two sides, and allows producing Janus particles in a large quantity.[35]

Pickering emulsion is commonly referred to emulsions that stabilized by solid particles rather than by low molecular weight surfactants.[36−38] The colloidal particles adsorbed at liquid−liquid interface can be functionalized in either the aqueous or oil phase, resulting in particles with two sides of different properties.[27−30] Granick and co-workers[27] have used the Pickering single emulsions to synthesize Janus particles with controllable geometry in gram-sized quantities. Typically they first created a wax-in-water Pickering emulsion using silica particles as stabilizers and then immobilized the silica particles at the wax−water interfaces through cooling down the emulsion temperature. Janus particles can be obtained after chemical modification on the aqueous side of the immobilized silica particles. More recently, Yang and co-workers[28] have reported the formation of Janus particles by simultaneous biphasic grafting of different polymer brushes onto the adsorbed particles at a liquid−liquid interface using atomic transfer radical polymerization (ATRP). In addition, Budhlall and co-workers[30] have reported a route to synthesize Janus particles containing laponite nanoclay armored with an anisotropic surface potential via two-step Pickering emulsion method. It is worthy noting that the above-mentioned approaches all employ single Pickering emulsions as templates. However, the information available on the use of double emulsions to generate Janus particles in the literature is scarce. Weitz and co-workers[39] have recently used microfluidic technique to produce Janus particles with a hydrophilic−organophilic structure templating from an oil-in-water-in-oil (O/W/O) double emulsion. However, the emulsions were stabilized by common surfactants, and the microfluidic technology has its intrinsic drawback; namely, the output is limited. Meanwhile, in spite of many synthetic strategies have been developed to fabricate novel materials with special

Received: January 7, 2013
Revised: April 6, 2013
Published: April 9, 2013

   dx.doi.org/10.1021/la400053g | *Langmuir* 2013, 29, 5138−5144

Scheme 1. Schematic Representation of the Developed Method for the Preparation of Janus Microspheres[a]

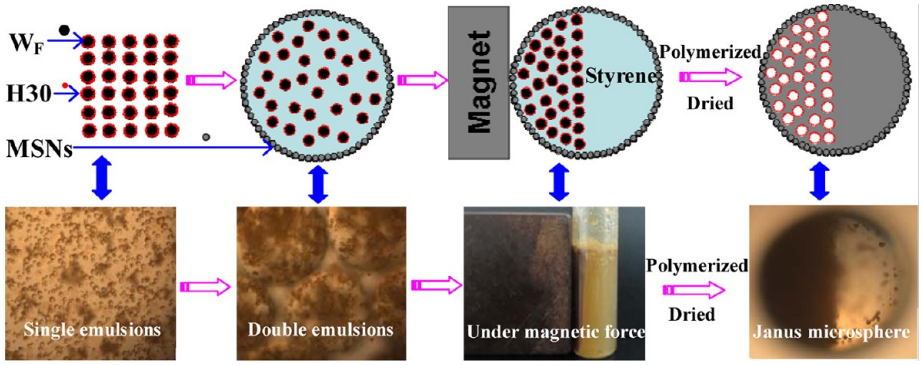

[a]Top row presents the cartoons while bottom row indicates the corresponding photographs.

structures and/or comprehensive properties, such as multihollow magnetic microspheres,[40] hollow Janus particles,[41] and magnetic Janus particles,[42,43] to our knowledge, the approach to produce multihollow magnetic microspheres with tunable distribution of the hollows inside the particles has not yet been reported.

Herein, we present a facile route for the preparation of Janus microparticles with dual anisotropy of porosity and magnetism based on Pickering-type double emulsions. The key advantage of this method is simple and enables to be scaled up for producing a large quantity of the final product. Meanwhile, it allows one to precisely control the interior structure of the Janus microspheres. In our previous work,[44] we have conceptually proved the availability of using Pickering double emulsions as templates for synthesizing the Janus microspheres. In this work, we examine in detail how to obtain such Janus microsphere with structural and magnetic anisotropy by focusing on the effects of Fe_3O_4 particle concentration, hydrophobic silica particle content, and volume ratio of the inner water phase to middle oil phase (W_F/O) on the Pickering double emulsion formation and consequently on the structure of the resulting Janus microspheres. In addition, the magnetic field induced orientation of the prepared Janus microsphere is demonstrated. Scheme 1 shows the process that has been used for the fabrication of the Janus microparticles with tunable interior structure. First, a stable aqueous Fe_3O_4 dispersion-in-oil-in-water ($W_F/O/W$) double Pickering emulsion was generated by using amorphous fumed silica powders (H30) and our recently synthesized mesoporous silica nanoparticles (MSNs, Figure S1 in the Supporting Information) as stabilizers for the primary inner W_F/O droplets and outer O/W droplets, respectively. Note that aqueous Fe_3O_4 dispersion (W_F, Figure S2) offers single emulsion droplets with magnetism, making them movable under a magnetic field. After that, polymerization of the middle oil phase of the double emulsions was started under an external magnetic field. Finally, the Janus microspheres with multihollow structure possessing magnetite nanoparticles concentrated within one side of the sphere were obtained after completing the polymerization.

EXPERIMENTAL SECTION

Materials. Ferric chloride hexahydrate ($FeCl_3{\cdot}6H_2O$), ferrous chloride tetrahydrate ($FeCl_2{\cdot}4H_2O$), cetyltrimethylammonium bromide (CTAB), tetraethoxysilane (TEOS), triethylamine (TEA), hydrochloric acid (HCl), ammonia, and ethanol are of analytical grade and used as received. Styrene (St, Guanghua Chemical Industries Co., China) was distilled under reduced pressure over CaH, and 2,2′-azobis(isobutyronitrile) (AIBN) was recrystallized from ethanol. Both of them were stored in the refrigerator before use. If not otherwise mentioned, all the reagents above were purchased from Shanghai Chemical Reagent Co. (China). The amorphous fumed silica powders (H30) with primary particle diameters between 5 and 30 nm were a gift from Wacker Chemie (Burghausen). Water used in all experiments was deionized and filtrated by a Millipore purification apparatus with resistivity more than 18.0 M cm.

Preparation of Single and Double Emulsions. Single emulsions (W_F/O) were produced by ultrasonic (100 W, 40 kHz) for 5 min after adding aqueous Fe_3O_4 dispersion into oil phase, which contains hydrophobic H30 as well as 1 wt % AIBN. After that, double emulsions ($W_F/O/W$) were generated by hand-shaking once the single emulsions were added into outer water phase possessing 0.4 wt % hydrophilic MSNs. We performed various series of emulsion preparations in the presence of different concentrations of Fe_3O_4 nanoparticles, contents of H30, and volume ratios of inner water phase to middle oil phase (W_F/O) in order to gain available recipe for the manufacture of the resulting Janus microspheres (see Table S1). In particular, we tuned the W_F/O volume ratio either by changing the aqueous phase (W_F) or the oil phase and investigated the effects on the final structure of the microspheres. Note that the amount of MSNs and volume ratio of (W_F/O)/W were kept at 0.4 wt % and 1:5, respectively, since they have shown less effect on the preparation of the target products, unless the amount of MSNs is not enough to emulsify the double emulsions.[45−47]

Polymerization of Double Emulsions. A permanent magnet was applied and fixed at the desired position of the double emulsions and polymerization was started by heating the system to 338 K for 24 h in an oven. The polymerization temperature was chosen at 338 K aiming to avoid the broken of double emulsions. After polymerization reaction, the as-prepared products were washed by ethanol several times, finally dried at 318 K.

Magnetic Orientation. First, Janus particles in dry condition were scattered onto a paper; thereafter, a permanent magnet was employed to approach on the top of them. These microparticles will stick with the magnet, and then a transparent adhesive tape was used to transport the microparticles off the magnet; finally, Janus particles with same arrangement can be detected with an optical microscope.

Characterization. The emulsions were observed with an optical microscope (Carl Zeiss, German). The inner structure of the microspheres was surveyed by scanning electron microscopy (SEM) with a Philips XL 30 at the acceleration voltage of 10 kV. The specimen was first scattered onto a conductive adhesive, then sliced by a razor blade under the observation of optical microscope, and finally sputtered with gold. Elemental analysis of the sample was conducted using an energy-dispersive X-ray (EDX) detector attached to the SEM to check the element composition of the as-prepared microspheres.

dx.doi.org/10.1021/la400053g | Langmuir 2013, 29, 5138−5144

RESULTS AND DISCUSSION

Effects of Fe_3O_4 Concentration on Emulsion Preparation. To simplify the preparation of magnetic single emulsions, we directly applied aqueous Fe_3O_4 dispersion (W_F, Figure S2) as inner water phase because it is time-saving and also we can easily obtain W_F/O emulsions with desired magnetic property compared with other magnetic emulsions stabilized by magnetite nanoparticles.[48−50]

Figure 1a−e presents the optical micrographs of W_F/O emulsions with different Fe_3O_4 concentrations ranging from 0

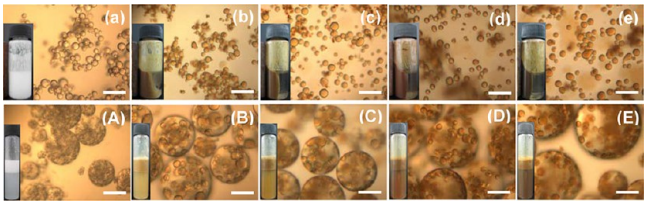

Figure 1. Optical micrographs of W_F/O emulsions (top row) and $W_F/O/W$ double emulsions (bottom row) with various Fe_3O_4 concentrations: (a, A) 0 mg mL^{-1}; (b, B) 10 mg mL^{-1}; (c, C) 20 mg mL^{-1}; (d, D) 30 mg mL^{-1}; and (e, E) 40 mg mL^{-1}. The insets of (a)−(e) indicate digital photos of single emulsion being attracted under an external magnetic force, and the insets of (A)−(E) displace digital photos of double emulsions in the absence of magnet. The H30 concentration and volume ratio of W_F/O were fixed at 0.3 wt % and 1:4, respectively. All scale bars present 50 μm.

to 40 mg mL^{-1}. As expected, the average diameter of the emulsions is all around 10 μm because emulsion diameter is mainly determined by the usage of H30 stabilizers when W_F/O ratio is fixed. From the insets of Figure 1a−e, we can observe that W_F/O emulsions cannot be effectively attracted to one side of the bottle when the Fe_3O_4 content is less than 30 mg mL^{-1}. In addition, the color of the W_F/O emulsions displays an obvious change, corresponding to the increasing of Fe_3O_4 concentration. More significantly, it shows that W_F/O emulsions are magnetized more easily and compactly with the increasing Fe_3O_4 concentration. However, the stability of the double emulsions is challenged by the ever-rising of the Fe_3O_4 concentration which can be distinctly observed in the insets of Figure 1A−E. It is apparent that the color of subnatant becomes darker and darker due to the emulsions breaking up, caused by shifting of Fe_3O_4 nanoparticles from inner water phase to outer water phase. To make a delicate balance between attractability of W_F/O droplets under the effect of a magnetic field and stability of the resulting double emulsions, we chose Fe_3O_4 concentration of 30 mg mL^{-1}. At this point, W_F/O emulsions can be side-assembled under the magnetic force, and the sequent $W_F/O/W$ double emulsions are stable enough upon polymerization.

Effects of H30 Content on Emulsion Preparation. Figure 2a−d shows the optical micrographs of W_F/O droplets with Fe_3O_4 concentration and W_F/O volume ratio fixed at 30 mg mL^{-1} and 1:4, respectively. H30 plays a critical role in controlling the droplet size and attractability of single emulsions. As can be seen in these graphs, average diameter of W_F/O emulsions is decreased from ~15 to ~2 μm along with increasing the H30 contents from 0.2 to 0.7 wt %. While, as shown in the insets of Figure 2a−d, W_F/O emulsions cannot be fully magnetized to one side of the bottle when the H30 content is above 0.5 wt % due to the increased W_F/O emulsion viscosity (see Figure S3).

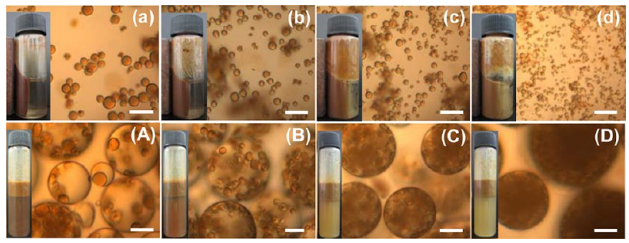

Figure 2. Optical micrographs of W_F/O emulsions (top row) and $W_F/O/W$ double emulsions (bottom row) with various H30 contents: (a, A) 0.2 wt %; (b, B) 0.3 wt %; (c, C) 0.5 wt %; and (d, D) 0.7 wt %. The insets of (a)−(d) indicate digital photos of single emulsions being attracted under an external magnetic force, and the insets of (A)−(D) displace digital photos of double emulsions in the absence of magnet. The Fe_3O_4 concentration and volume ratio of W_F/O were fixed at 30 mg mL^{-1} and 1:4, respectively. All scale bars present 50 μm.

Figure 2A−D reveals that $W_F/O/W$ emulsions become more and more opaque as the H30 content increases from 0.2 to 0.7 wt %. This phenomenon is likely caused by the decreased inner droplet size and also the better dispersion of the droplets, which subsequently decrease the light transmittance of double emulsions. The insets of Figure 2A−D demonstrate the effect of H30 content on the stability of double emulsions. The double emulsions become unstable when the H30 content is lower than 0.2 wt %, which could be easily found from the color changes of the subnatants, caused by broken of the double emulsions. Obviously, with H30 content of 0.3 wt %, it can simultaneously satisfy the attractability of single emulsion and stability of the sequent double emulsions.

Effects of W_F/O Volume Ratio on Emulsion Preparation. We employed two routes to vary the W_F/O volume ratio. The first approach discussed here was to fix the Fe_3O_4 concentration, the H30 content, and the middle oil volume as constant while the amount of aqueous Fe_3O_4 dispersion was varied. The W_F/O volume ratio changed by varying the volume of oil phase will be discussed in the next section. The dark agglomerations shown in Figure 3c suggest that W_F/O emulsions become unstable when the W_F/O volume ratio is increased to 1:3. This result reveals that with increasing the volume of aqueous Fe_3O_4 dispersion, the fixed amount of H30 particles become insufficient to cover the increased interfacial areas, resulting in the destabilization of the emulsions. The

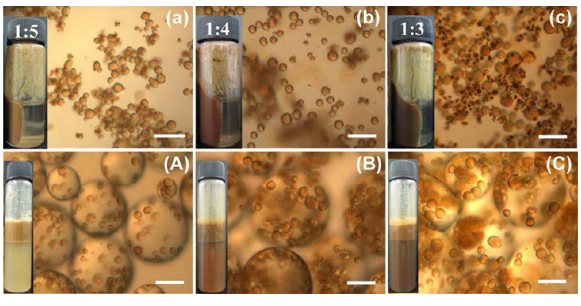

Figure 3. Optical micrographs of W_F/O emulsions (top row) and $W_F/O/W$ double emulsions (bottom row) with various W_F/O volume ratios: (a, A) 1:5; (b, B) 1:4; and (c, C) 1:3. The insets of (a)−(c) present digital photos of single emulsions being attracted under an external magnetic force, and the insets of (A)−(C) show digital photos of double emulsions in the absence of magnet. The Fe_3O_4 concentration and H30 content were fixed at 30 mg mL^{-1} and 0.3 wt %, respectively. All scale bars present 50 μm.

dx.doi.org/10.1021/la400053g | Langmuir 2013, 29, 5138−5144

insets of Figure 3a–c show that the volume of side-assembled W_F/O emulsions is enhanced with the increasing of W_F/O volume ratio from 1:5 to 1:3, and the color of W_F/O emulsions becomes darker. Meanwhile, remarkable double emulsions breaking-up can be observed as W_F/O volume ratio increased in Figure 3A–C. Generally, it is expected that the final microparticles with different distribution of voids (named Janus balance) can be obtained by adjusting the W_F/O volume ratio in precursor emulsions. However, this route cannot reach that goal because it is difficult to make a delicate balance between the W_F/O volume ratio and stability of the double emulsions.

Porous Anisotropy of Janus Microspheres. Figure 4 shows the optical micrographs and SEM images of the resulting

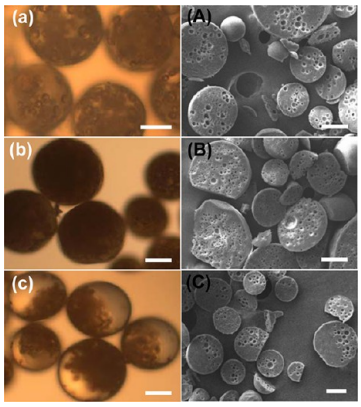

Figure 4. Optical micrographs (left column) and SEM images (right column) of the microspheres obtained after polymerization of the middle oil phase of the double emulsions under different conditions: (a, A) in the absence of Fe_3O_4 nanoparticles; (b, B) with a high H30 concentration of 0.7 wt %; (c, C) Fe_3O_4 concentration, H30 content, and W_F/O ratio are fixed at 30 mg mL^{-1}, 0.3 wt %, and 1:4, respectively. All scale bars represent 50 μm.

microspheres after polymerization of the middle oil phase of the double emulsions under different conditions. By comparing the optical micrographs, it is clear to see that there are distinct differences between non-Janus microspheres and Janus microspheres. For non-Janus microspheres, opaque small spheres are randomly distributed within the big spheres, while for Janus one, opaque small spheres are side-concentrated inside the big spheres (Figure 4a–c). As expected, the target microspheres cannot be produced without introducing the Fe_3O_4 nanoparticles. Small voids are randomly distributed within the big microspheres in the absence of Fe_3O_4 nanoparticles (Figure 4a,A). Meanwhile, at the 0.7 wt % H30, smaller voids are also disorderly distributed inside the microspheres (Figure 4b,B) in spite of the presence of Fe_3O_4 nanoparticles. This is because single emulsions cannot be side-attracted when H30 content is too high as mentioned above (inset in Figure 2d). It demonstrates that if we want to drive the single emulsion droplets to one side of the double emulsions, first of all, we need to make sure single emulsion droplets are drivable. Figure 4C provides the direct evidence that the small pores, which seem like solid black spheres in Figure 4c, are side-concentrated in the big solid spheres. It is worth noting that the size distribution discrepancy is observed by comparison of optic photographs and SEM images. This is caused by randomly slicing the samples during the SEM specimen preparation. At the same time, hemispheres with homogeneous distributed pores are detected (in Figure 4C). This is because only the multihollow part of microspheres is cut during the SEM sample preparation.

On the basis of the aforementioned observation, we can summarize that the synthesis method is simple, but it is crucial to choose the proper recipe. To manufacture the Janus microspheres successfully, two prerequisites are needed to be simultaneously satisfied. On one hand, the inner droplets should be attractable, which is fulfilled by utilizing aqueous Fe_3O_4 dispersion with desirable Fe_3O_4 concentration. At the same time, the viscosity of the inner W_F/O emulsions should be carefully tuned by adjusting the H30 content. On the other hand, the stability of the single emulsions and the double emulsions needs to be maintained under the conditions of both polymerization temperature and applying external magnetic force.

Controlling the Interior Structure of the Janus Microspheres. The distribution of the multihollow structure (e.g., Janus balance) of the microspheres can be tuned by varying the W_F/O ratio. This can be achieved either by changing the amount of aqueous Fe_3O_4 dispersion or the dosage of oil phase. As mentioned above, varying the amount of aqueous Fe_3O_4 dispersion may lead to the destabilization of the resulting double emulsions. In line of this, we varied the oil dosage to control the Janus balance inside the resulting microspheres.

Figure 5 shows the as-prepared anisotropic microspheres with different distribution of the multihollow inside the microspheres. It can be seen that the volume of multihollow part increases gradually as the W_F/O volume ratio increases from 1:10 to 1:2. Meanwhile, the multihollow part becomes

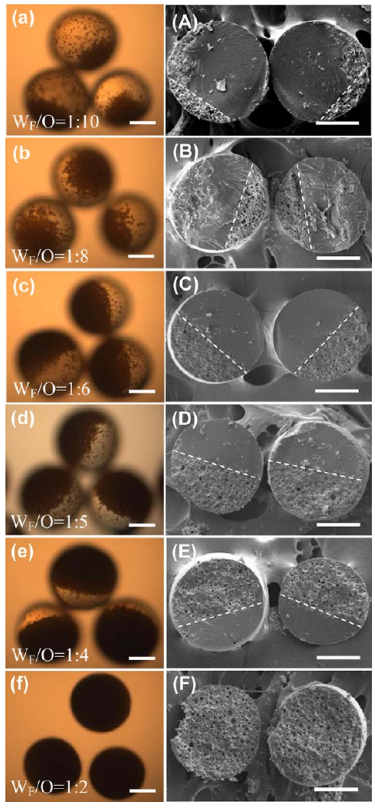

Figure 5. Optical micrographs (left column) and the corresponding SEM images (right column) of microspheres produced under various W_F/O volume ratios. All scale bars represent 150 μm.

dx.doi.org/10.1021/la400053g | *Langmuir* 2013, 29, 5138–5144

darker and darker due to the diffuse scattering caused by the increased voids in the microsphere. From the corresponding SEM images, it is clear to see the precise distribution of voids within the big microspheres under different W_F/O ratio conditions. A Janus microsphere, roughly half-occupied by voids (Figure 5C–E), can be obtained when W_F/O volume ratio is set ranging from 1:6 to 1:4, but the optimum W_F/O volume ratio goes to 1:5.

Is it possible to get the target products with desired distribution of the voids? Our results demonstrate that it is feasible. Before answer this question in details, we need to figure out the relationship between distribution of the voids and W_F/O volume ratio when other parameters are fixed. Actually, the distribution of the voids depends on the relative volume of multihollow part and solid part in each microsphere. Therefore, we first calculate the relative volume of multihollow part and solid part ($V_{multihollow}/V_{solid}$) of the Janus microsphere prepared under different W_F/O volume ratios, and then we can indirectly obtain the relationship between distribution of the voids and W_F/O volume ratio (see details in the Supporting Information):

$$\frac{V_{h,e}}{V_{H,e}} = \frac{h^2(3R - h)}{H^2(3R - H)} \quad (1)$$

$$\frac{V_{h,t}}{V_{H,t}} = \frac{1}{0.74\gamma - 0.26} \quad (2)$$

where h and H express the hemispherical heights, R is the radius of the Janus microsphere, $V_{h,e}$ and $V_{H,e}$ represent the experimental volume of spherical segment with a height of h and H, respectively, $V_{h,t}$ and $V_{H,t}$ present the theoretical volume of spherical segment with a height of h and H, respectively, and γ indicates the ratio value of O/W_F.

In eq 1, $V_{h,e}/V_{H,e}$ can be directly obtained by measuring the height of multihollow part and solid part of the prepared Janus microspheres (see Scheme 2), while $V_{h,t}/V_{H,t}$ can be deduced

Scheme 2. Schematic Representation of Janus Microsphere

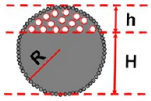

based on maximum packing fraction theory. For a high internal phase emulsion (HIPE), the maximum packing fraction of the monodispersed spheres is 0.74.[51] Accordingly, we assumed that all single emulsion droplets are of same size and closely packed within one side of double emulsion droplets; then we can achieve the relationship between $V_{h,t}/V_{H,t}$ and W_F/O volume ratio as shown in eq 2.

Figure 6 shows the relationship between $V_{h,e}/V_{H,e}$ and $V_{h,t}/V_{H,t}$ under various W_F/O volume ratios (see data summary in the Supporting Information). Interestingly, at the point of W_F/O volume ratio of 1/10, $V_{h,e}/V_{H,e}$ is slightly smaller than $V_{h,t}/V_{H,t}$. However, after that the experimental values are always larger than the theoretically calculated values. This can be attributed to the fact that the droplets are deformable under this condition, in which the previously spherical droplets are flattened in the areas of close contact of neighboring voids (see Figure 5A). When W_F/O volume ratio is larger than 1/8, $V_{h,e}/V_{H,e}$ deviates from $V_{h,t}/V_{H,t}$ significantly along with the increasing W_F/O volume ratio. This suggests that the pores

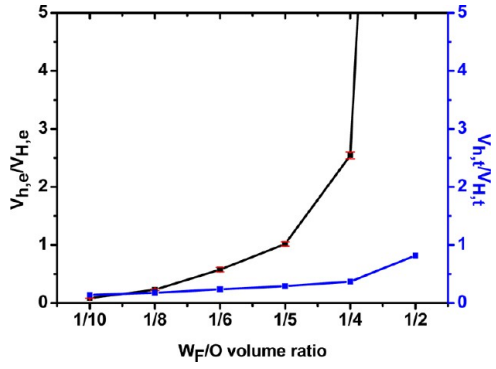

Figure 6. Relationship between $V_{h,e}/V_{H,e}$ and $V_{h,t}/V_{H,t}$ under different conditions of W_F/O volume ratios. The black line demonstrates the relationship between $V_{h,e}/V_{H,e}$ and W_F/O volume ratio, while the blue line shows the relationship between $V_{h,t}/V_{H,t}$ and W_F/O volume ratio.

are not closely packed but with a certain distance, which can be confirmed from the SEM images. This effect is enhanced with increasing the W_F/O volume ratio due to the increased viscosity of W_F/O emulsions. In the present study, H30 content was fixed, but the relative concentration of H30 in oil phase would rise when the dosage of oil phase was decreased, resulting in the increase of the viscosity of W_F/O emulsions.

Thus, through comparing the difference of $V_{h,e}/V_{H,e}$ and $V_{h,t}/V_{H,t}$, we can indirectly get the information on voids compactness. Meanwhile, by checking the relationship between $V_{h,e}/V_{H,e}$ and W_F/O volume ratio, we can facilely and precisely fabricate the microspheres of any Janus balance we want by choosing the corresponding W_F/O volume ratio.

Magnetic Anisotropy and Magnetic Orientation. Figure S4 illuminates the asymmetric distribution of elements within the Janus microsphere. The multihollow part is composed of C, O, Si, and Fe while the solid side displaced of C, O, and Si, indicating that Fe_3O_4 nanoparticles did not migrate to oil phase during the double emulsion preparation and polymerization process. Moreover, H30 nanoparticles were not completely absorbed onto W_F/O interface but partly dispersed within the oil phase, which explain why Si and O elements can be detected in solid part of the sphere. Compared with Dyab's work,[42] our method is much easier and based on attracting magnetic droplets to side-assemble within one side of the double emulsions, which leads to not only more complicated inner structure but also absolute magnetic anisotropy.

As shown in Figure S5, saturation magnetization (Ms) for the prepared Janus microspheres is 0.32 emu g^{-1}, which is much smaller than bulk magnetite nanoparticles (see the inset in Figure S2b). This is because Ms is directly proportional to the volume fraction of the particles and the saturation moment of a single particle.[52,53] It could be considered that the saturation magnetization of the microspheres depends mainly on the volume fraction of the Fe_3O_4 particles, due to the nonmagnetic polystyrene contribution to the total magnetization, resulting in the decrease of the saturation magnetization. Ever though their Ms is only 0.32 emu g^{-1}, the as-prepared Janus microspheres can be easily magnetized under an external magnetic force.[44]

Because of the special internal structure and magnetic anisotropy, the as-prepared Janus microspheres can be magnetically orientated. Before orientation, Janus microparticles are in disorganized form (Figure 7a,b), while after magnetic orientation, well-orientated Janus microparticles with

dx.doi.org/10.1021/la400053g | Langmuir 2013, 29, 5138–5144

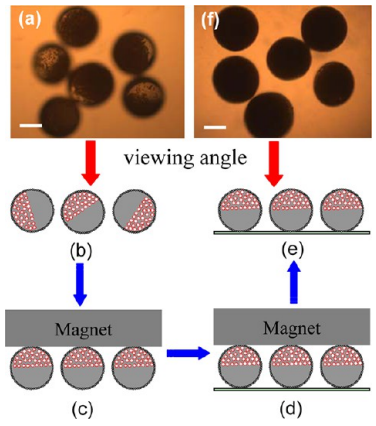

Figure 7. (a) Optical micrograph of Janus microspheres before orientation (sample 13, Table S1); (b) random pattern; (c) Janus microspheres being orientated under a magnet; (d) transporting onto a transparent adhesive tape; (e) orientated Janus microspheres being attached on a transparent adhesive tape; (f) optical micrograph of the orientated Janus microspheres. The scale bar represents 150 μm.

multihollow part on the same side can be detected by optical microscope (Figure 7f). Figure 7c,d shows the process of how to orientate the as-prepared Janus microparticles. Before taking Figure 7f, all these Janus microspheres were orientated under an external magnetic field (Figure 7c), making their multihollow part closely attached to the magnet since multihollow part possess magnetite particles which are preferentially to stick with the magnet. Then, these orientated Janus spheres were transferred to a transparent adhesive tape (Figure 7d), and finally the photographs were taken. Figure 7f appears that the Janus microspheres are opaque since they are photographed with solid part down while multihollow part up as shown in Figure 7e, and a detailed schematic diagram can be found in Figure S6. For the purpose of comparison, we also examine the magnetic orientation of other Janus microspheres with different voids distribution (see Figure S7). Inspired by its magnetic orientation property, we conjecture that Janus membrane can be fabricated through arranging the orientated Janus microspheres under proper conditions.

CONCLUSIONS

We have fabricated a novel type of Janus microsphere with structural anisotropy and magnetic asymmetry, in which the multihollow structure possessing magnetite nanoparticles are side-assembled within one part of the microspheres. Importantly, we successfully demonstrated that the distribution of the voids inside the microsphere can be facilely and precisely tuned by varying the W_F/O volume ratio. The as-prepared Janus microspheres can be magnetically orientated due to the special internal structure and magnetic asymmetric distribution. It may have potential applications in the areas of biomedical system, asymmetric catalysis, and one-side drug delivery. Besides, its magnetic orientation property makes it a good candidate for synthesizing Janus membrane.

ASSOCIATED CONTENT

Supporting Information

Summary of synthetic conditions for the preparation of the Janus microspheres, the summary of $V_{h,t}/V_{H,t}$ and $V_{h,e}/V_{H,e}$ as a function of WF/O ratio, preparation and discussion of mesoporous silica nanoparticles (MSNs) and aqueous Fe_3O_4 dispersion (W_F), single emulsion viscosity, formula derivation, magnetic anisotropy, magnetization curve of Janus microspheres, schematic diagram for Janus microsphere detected from different viewing angle, and comparison of nonorientated Janus microsphere with orientated Janus microsphere. This material is available free of charge via the Internet at http://pubs.acs.org.

AUTHOR INFORMATION

Corresponding Author

*E-mail: zhywang@scut.edu.cn (C.W.); tongai@cuhk.edu.hk (T.N.).

Notes

The authors declare no competing financial interest.

ACKNOWLEDGMENTS

This work was supported by the National Basic Research Program of China (973 Program, 2012CB821500), the National Natural Science Foundation of China (21274046), the Natural Science Foundation of Guangdong Province (S20120011057), and the Hong Kong Special Administration Region (HKSAR) General Research Fund (CUHK403210, 2130237).

REFERENCES

(1) Nisisako, T.; Torii, T.; Takahashi, T.; Takizawa, Y. Synthesis of Monodisperse Bicolored Janus Particles with Electrical Anisotropy Using a Microfluidic Co-Flow System. *Adv. Mater.* **2006**, *18*, 1152−1156.

(2) Wurm, F.; Kilbinger, A. F. M. Polymeric Janus Particles. *Angew. Chem., Int. Ed.* **2009**, *48*, 8412−8421.

(3) Glaser, N.; Adams, D. J.; Böker, A.; Krausch, G. Janus Particles at Liquid-Liquid Interfaces. *Langmuir* **2006**, *22*, 5227−5229.

(4) Ruhland, T. M.; Gröschel, A. H.; Walther, A.; Müller, A. H. E. Janus Cylinders at Liquid−Liquid Interfaces. *Langmuir* **2011**, *27*, 9807−9814.

(5) Walther, A.; Matussek, K.; Müller, A. H. E. Engineering Nanostructured Polymer Blends with Controlled Nanoparticle Location using Janus Particles. *ACS Nano* **2008**, *2*, 1167−1178.

(6) McConnell, M. D.; Kraeutler, M. J.; Yang, S.; Composto, R. J. Patchy and Multiregion Janus Particles with Tunable Optical Properties. *Nano Lett.* **2010**, *10*, 603−609.

(7) Glotzer, S. C.; Solomon, M. J. Anisotropy of Building Blocks and Their Assembly into Complex Structures. *Nat. Mater.* **2007**, *6*, 557−562.

(8) Walther, A.; Drechsler, M.; Müller, A. H. E. Structures of Amphiphilic Janus Discs in Aqueous Media. *Soft Matter* **2009**, *5*, 385−390.

(9) Walther, A.; Drechsler, M.; Rosenfeldt, S.; Harnau, L.; Ballauff, M.; Abetz, V.; Müller, A. H. E. Self-assembly of Janus Cylinders into Hierarchical Superstructures. *J. Am. Chem. Soc.* **2009**, *131*, 4720−4728.

(10) Yuet, K. P.; Hwang, D. K.; Haghgooie, R.; Doyle, P. S. Multifunctional Superparamagnetic Janus Particles. *Langmuir* **2009**, *26*, 4281−4287.

(11) Jiang, S.; Chen, Q.; Tripathy, M.; Luijten, E.; Schweizer, K. S.; Granick, S. Janus Particle Synthesis and Assembly. *Adv. Mater.* **2010**, *22*, 1060−1071.

(12) Howse, J. R.; Jones, R. A. L.; Ryan, A. J.; Gough, T.; Vafabakhsh, R.; Golestanian, R. Self-motile Colloidal Particles: from Directed Propulsion to Random Walk. *Phys. Rev. Lett.* **2007**, *99*, 048102.

(13) Takei, H.; Shimizu, N. Gradient Sensitive Microscopic Probes Prepared by Gold Evaporation and Chemisorption on Latex Spheres. *Langmuir* **1997**, *13*, 1865−1868.

(14) Paunov, V. N.; Cayre, O. J. Supraparticles and "Janus" Particles Fabricated by Replication of Particle Monolayers at Liquid Surfaces Using a Gel Trapping Technique. *Adv. Mater.* **2004**, *16*, 788−791.

(15) Lu, Y.; Xiong, H.; Jiang, X. C.; Xia, Y. N.; Prentiss, M.; Whitesides, G. M. Asymmetric Dimers Can Be Formed by Dewetting Half-Shells of Gold Deposited on the Surfaces of Spherical Oxide Colloids. *J. Am. Chem. Soc.* **2003**, *125*, 12724−12725.
(16) Suzuki, D.; Kawaguchi, H. Janus Particles with a Functional Gold Surface for Control of Surface Plasmon Resonance. *Colloid Polym. Sci.* **2006**, *284*, 1471−1476.
(17) Roh, K. H.; Martin, D. C.; Lahann, J. Biphasic Janus Particles with Nanoscale Anisotropy. *Nat. Mater.* **2005**, *4*, 759−763.
(18) Koo, H. Y.; Yi, D. K.; Yoo, S. J.; Kim, D. Y. A Snowman-like Array of Colloidal Dimers for Antireflecting Surfaces. *Adv. Mater.* **2004**, *16*, 274−277.
(19) Li, Z. F.; Lee, D. Y.; Rubner, M. F.; Cohen, R. E. Layer-by-Layer Assembled Janus Microcapsules. *Macromolecules* **2005**, *38*, 7876−7879.
(20) Erhardt, R.; Boeker, A.; Zettl, H.; Kaya, H.; Pyckhout-Hintzen, W.; Krausch, G.; Abetz, V.; Mueller, A. H. E. Janus Micelles. *Macromolecules* **2001**, *34*, 1069−1075.
(21) Erhardt, R.; Zhang, M.; Boeker, A.; Zettl, H.; Abetz, C.; Frederik, P.; Krausch, G.; Abetz, V.; Mueller, A. H. E. Amphiphilic Janus Micelles with Polystyrene and Poly(methacrylic acid) Hemispheres. *J. Am. Chem. Soc.* **2003**, *125*, 3260−3267.
(22) Voets, I. K.; Fokkink, R.; Hellweg, T.; King, S. M.; de Waard, P.; de Keizer, A.; Cohen Stuart, M. A. Spontaneous Symmetry Breaking: Formation of Janus Micelles. *Soft Matter* **2009**, *5*, 999−1005.
(23) Zhang, J.; Wang, X. J.; Wu, D. X.; Liu, L.; Zhao, H. Y. Bioconjugated Janus Particles Prepared by in Situ Click Chemistry. *Chem. Mater.* **2009**, *21*, 4012−4018.
(24) Dendukuri, D.; Doyle, P. S. The Synthesis and Assembly of Polymeric Microparticles using Microfluidics. *Adv. Mater.* **2009**, *21*, 4071−4086.
(25) Nie, Z. H.; Li, W.; Seo, M.; Xu, S. Q.; Kumacheva, E. Janus and Ternary Particles Generated by Microfluidic Synthesis: Design, Synthesis, and Self-assembly. *J. Am. Chem. Soc.* **2006**, *128*, 9408−9412.
(26) Shepherd, R. F.; Conrad, J. C.; Rhodes, S. K.; Link, D. R.; Marquez, M.; Weitz, D. A.; Lewis, J. A. Microfluidic Assembly of Homogeneous and Janus Colloid-filled Hydrogel Granules. *Langmuir* **2006**, *22*, 8618−8622.
(27) Hong, L.; Jiang, S.; Granick, S. Simple Method to Produce Janus Colloidal Particles in a Large Quantity. *Langmuir* **2006**, *22*, 9495−9499.
(28) Liu, B.; Wei, W.; Qu, X. Z.; Yang, Z. Z. Janus Colloids Formed by Biphasic Grafting at a Pickering Emulsion Interface. *Angew. Chem., Int. Ed.* **2008**, *120*, 4037−4039.
(29) Zhang, J.; Jin, J.; Zhao, H. Y. A One-Step Approach for the Synthesis of Amphiphilic Janus Silica Particles. *Langmuir* **2009**, *25*, 6431−6437.
(30) Pardhy, N. P.; Budhlall, B. M. Pickering Emulsion as a Template to Synthesize Janus Colloids with Anisotropy in the Surface Potential. *Langmuir* **2010**, *26*, 13130−13141.
(31) Chen, Y.; Liang, F. X.; Yang, H. L.; Zhang, C. L.; Wang, Q.; Qu, X. Z.; Li, J. L.; Cai, Y. L.; Qiu, D.; Yang, Z. Z. Janus Nanosheets of Polymer-Inorganic Layered Composites. *Macromolecules* **2012**, *45*, 1460−1467.
(32) Zhou, T.; Wang, B. B.; Dong, B.; Li, C. Y. Thermoresponsive Amphiphilic Janus Silica Nanoparticles via Combining "Polymer Single-Crystal Templating" and "Grafting-from" Methods. *Macromolecules* **2012**, *45*, 8780−8789.
(33) Wang, Y. H.; Zhang, C. L.; Tang, C.; Li, J.; Shen, K.; Liu, J. G.; Qu, X. Z.; Li, J. L.; Wang, Q.; Yang, Z. Z. Emulsion Interfacial Synthesis of Asymmetric Janus Particles. *Macromolecules* **2011**, *44*, 3787−3794.
(34) Liu, B.; Liu, J. G.; Liang, F. X.; Wang, Q.; Zhang, C. L.; Qu, X. Z.; Li, J. L.; Qiu, D.; Yang, Z. Z. Robust Anisotropic Composite Particles with Tunable Janus Balance. *Macromolecules* **2012**, *45*, 5176−5184.
(35) Jiang, S.; Chen, Q.; Tripathy, M.; Luijten, E.; Schweizer, K. S.; Granick, S. Janus Particle Synthesis and Assembly. *Adv. Mater.* **2010**, *22*, 1060−1071.
(36) Ramsden, W. Separation of Solids in the Surface-Layers of Solutions and "Suspensions". *Proc. R. Soc. London* **1903**, *72*, 156−164.
(37) Pickering, S. U. Emulsions. *J. Chem. Soc.* **1907**, *91*, 2001−2021.
(38) Fujii, S.; Cai, Y. L.; Weaver, J. V. M; Armes, S. P. Syntheses of Shell Cross-linked Micelles Using Acidic ABC Triblock Copolymers and Their Application as pH-Responsive Particulate Emulsifiers. *J. Am. Chem. Soc.* **2005**, *127*, 7304−7305.
(39) Chen, C. H.; Shah, R. K.; Abate, A. R.; Weitz, D. A. Janus Particles Templated from Double Emulsion Droplets Generated Using Microfluidics. *Langmuir* **2009**, *25*, 4320−4323.
(40) Yang, S.; Liu, H. R.; Zhang, Z. C. Fabrication of Novel Multihollow Superparamagnetic Magnetite/Polystyrene Nanocomposite Microspheres via Water-in-Oil-in-Water Double Emulsions. *Langmuir* **2008**, *24*, 10395−10401.
(41) Tang, C.; Zhang, C. L.; Liu, J. G.; Qu, X. Z.; Li, J. L.; Yang, Z. Z. Large Scale Synthesis of Janus Submicrometer Sized Colloids by Seeded Emulsion Polymerization. *Macromolecules* **2010**, *43*, 5114−5120.
(42) Dyab, A. K. F.; Ozmen, M.; Ersoz, M.; Paunov, V. N. Fabrication of Novel Anisotropic Magnetic Microparticles. *J. Mater. Chem.* **2009**, *19*, 3475−3481.
(43) Rahman, M. M.; Montagne, F.; Fessi, H.; Elaissari, A. Anisotropic Magnetic Microparticles from Ferrofluid Emulsion. *Soft Matter* **2011**, *7*, 1483−1490.
(44) Ning, Y.; Wang, C. Y.; Ngai, T.; Yang, Y.; Tong, Z. Hollow Magnetic Janus Microspheres Templated from Double Pickering Emulsions. *RSC Adv.* **2012**, *2*, 5510−5512.
(45) Bon, S. A. F.; Cauvin, S.; Colver, P. J. Colloidosomes as Micron-Sized Polymerisation Vessels to Create Supracolloidal Interpenetrating Polymer Network Reinforced Capsules. *Soft Matter* **2007**, *3*, 194−199.
(46) Chen, T.; Colver, P. J.; Bon, S. A. F. Organic-Inorganic Hybrid Hollow Spheres Prepared from TiO_2-Stabilized Pickering Emulsion Polymerization. *Adv. Mater.* **2007**, *19*, 2286−2289.
(47) Aveyard, R.; Binks, B. P.; Clint, J. H. Emulsions Stabilised Solely by Colloidal Particles. *Adv. Colloid Interface Sci.* **2003**, *100−102*, 503−546.
(48) Zhou, J.; Qiao, X. Y.; Binks, B. P.; Sun, K.; Bai, M. W.; Li, Y. L.; Liu, Y. Magnetorheological Behavior of Pickering Emulsions Stabilized by Surface-Modified Fe_3O_4 Nanoparticles. *Langmuir* **2011**, *27*, 3308−3316.
(49) Xiao, Q.; Tan, X. K.; Ji, L. L.; Xue, J. Preparation and Characterization of Polyaniline/Nano-Fe_3O_4 Composites via a Novel Pickering Emulsion Route. *Synth. Met.* **2007**, *157*, 784−791.
(50) Liu, H. X.; Wang, C. Y.; Gao, Q. X.; Liu, X. X.; Tong, Z. Magnetic Hydrogels with Supracolloidal Structures Prepared by Suspension Polymerization Stabilized by Fe_2O_3 Nanoparticles. *Acta Biomater.* **2010**, *6*, 275−281.
(51) Cameron, N. R.; Sherrington, D. C. High Internal Phase Emulsions: Structure, Properties and Use in Polymer Preparation. *Adv. Polym. Sci.* **1996**, *126*, 163−214.
(52) Bacri, J. C.; Perzynski, R.; Salin, D.; Cabuil, V.; Massart, R. Magnetic Colloidal Properties of Ionic Ferrofluids. *J. Magn. Mater.* **1986**, *62*, 36−46.
(53) Sauzedde, F.; Elaissari, A.; Pichot, C. Hydrophilic Magnetic Polymer Latexes. 1. Adsorption of Magnetic Iron Oxide Nanoparticles onto Various Cationic Latexes. *Colloid Polym. Sci.* **1999**, *277*, 846−855.